Statistical Models in Morphometrics: Are They Realistic?

Subhash Lele; Joan T. Richtsmeier

Systematic Zoology, Vol. 39, No. 1. (Mar., 1990), pp. 60-69.

Stable URL:
http://links.jstor.org/sici?sici=0039-7989%28199003%2939%3A1%3C60%3ASMIMAT%3E2.0.CO%3B2-G

Systematic Zoology is currently published by Society of Systematic Biologists.

Syst. Zool., 39(1):60-69, 1990

STATISTICAL MODELS IN MORPHOMETRICS: ARE THEY REALISTIC?*

SUBHASH LELE[1] AND JOAN T. RICHTSMEIER[2]

[1]*Department of Biostatistics, The Johns Hopkins University, School of Hygiene and Public Health, Baltimore, Maryland 21205*
[2]*Department of Cell Biology and Anatomy, The Johns Hopkins University School of Medicine, Baltimore, Maryland 21205*

Abstract.—This analysis considers the validity of the assumptions of the Gaussian perturbation model as applied to landmark data collected for morphometric analyses. The primary conclusion is that the assumption of homoscedasticity is unrealistic when applied to biological data sets. We also point out some important difficulties associated with alternate models. [Perturbation models; models for linear distances.]

Morphometrics is the quantitative analysis of size and shape. Recent years are marked by the development of new statistical methods and models for the study of size, shape and also shape differences between populations of forms (e.g., Bookstein et al. 1985, Bookstein 1986, 1989a, b, and references therein; Goodall and Bose, 1987). We focus here on methods used to analyze landmark data. A statistical model that is commonly used in the development of statistical procedures is the Gaussion perturbation model. A basic assumption of this model as proposed by Bookstein (1984) is that variability around each landmark is constant throughout the object.

The purpose of this paper is to examine this assumption using actual data sets collected for morphometric analyses. Our conclusion is that real data sets do not necessarily concur with the assumption of constant variability local to landmarks. We also point out difficulties associated with some alternate models suggested in the literature. Our results underscore the need for developing models which are more flexible, and consequently more realistic. Though technical in nature, we feel the conclusions of this paper are important for biologists and scientists who use these models for morphometric analysis.

*This is Technical Report #687 from the Department of Biostatistics, The Johns Hopkins University.

In the following sections, we briefly describe the perturbation model, closely following the description and notation of Goodall and Bose (1987). We then introduce the data sets and present the results of our analyses. Finally, we discuss some alternate models and point out the difficulties associated with them.

GAUSSIAN PERTURBATION MODEL

Let $X_1, X_2, \ldots, X_L$ be $N \times K$ matrices of the coordinates of N landmarks in R^K. K may equal 2 or 3. Each form, X_i, is modeled as a similarity transformation of a random first order normal perturbation of the mean unknown population X,

$$X_i = b_i(X + E_i)R_i + 1_N t_i^T \qquad (1)$$

where

$$E_i = \epsilon Z_i^X + 0(\epsilon^2)$$

and $\epsilon > 0$ is small; the Z_i^X: $N \times K$ are independent matrices of independent identically distributed N(0, 1) random variables; $b_i > 0$ is a scaler; R_i: $K \times K$ is an orthogonal matrix; and t_i: $K \times 1$ is a vector. The triplet (b_i, R_i, t_i) specifies the dilation, rotation and translation components of the similarity transformation of the E_i perturbed X. ϵ specifies the variability around each landmark and is constant throughout the object. The reader may refer to Book-

TABLE 1. Two-dimensional landmarks used in analysis of Crouzon, Apert, and normal individuals.

Landmark number	Landmark name and description
1	Nasion. Point of intersection of the nasal bones with the frontal bone.
2	Nasale. Inferior-most point of intersection of the nasal bones.
3	Anterior nasal spine. Anterior-most point at the medial intersection of the maxillary bones at the base of the nasal aperture.
4	Intradentale superior. The point is located on the alveolar border of the maxilla between the central incisors.
5	Posterior nasal spine. Posterior-most point of intersection of the right and left palatal shelves.
6	Tuberculum sella. "Saddle" of bone just posterior to the chiasmatic groove on the body of the sphenoid bone.
7	Sella. Most inflexive point of the hypophyseal fossa. The hypophyseal (pituitary) fossa is defined as the bony depression which holds the pituitary gland. This fossa is bounded by tuberculum sella anteriorly and posterior sella posteriorly.
8	Posterior sella. A square plate of bone which serves as the posterior border of the hypophyseal fossa.
9	Basion. The most anterior border of the foramen magnum.
10	Internal occipital protuberance of the cruciate eminence of the occipital bone.

stein (1986:fig. 2) for a pictoral representation of this model in the case of two-dimensional data.

IMPLICATIONS OF THE MODEL

There are two important implications of the model briefly outlined above.

First, the value of ϵ is constrained, perhaps severely. In most landmark based, biological data sets, it is unlikely that two landmarks would switch their relative positions within a biologically homogeneous group. Proper representation of this reality requires that the variability around the landmarks be "considerably smaller" than the distances between the landmarks (see Bookstein, 1986:137). If one assumes that this variability is constant throughout the object, then ϵ must be considerably smaller than the smallest distance between any pair of landmarks. If the biological object under consideration is characterized by a few landmarks that are close together and others that are further spread apart, then the value of ϵ is severely restricted by the distances between the more closely spaced landmarks.

Second, assuming constancy of variability around landmarks across a biological form implies equal variances among biological regions within the forms. It follows that, if we split the object in two (or more) parts, the estimate of ϵ obtained by analyzing the sections separately should be similar.

This concept can be examined in a way that is similar to the technique of checking the assumption of homoscedasticity in regression analysis. In regression, the data are split into two parts and σ^2 is estimated by S_1^2 and S_2^2. If S_1^2 and S_2^2 are close, the assumption of homoscedasticity may hold; otherwise, it is suspect.

In the following section, we describe biological data sets which we use to examine these implications more closely.

DESCRIPTION OF THE BIOLOGICAL DATA

The first data set consists of two-dimensional landmark coordinates digitized from lateral radiographs of normal children and those affected with two genetic syndromes, Crouzon syndrome and Apert syndrome. The Crouzon and Apert samples come from patient records of the Center for Craniofacial Anomalies, Chicago. None of the syndromic individuals had undergone craniofacial surgery. The normal sample is from the Bolton-Brush Growth Study (Broadbent et al., 1975). Details of original data collection procedures can be found in Richtsmeier (1985).

In this study, we use 10 landmarks (Ta-

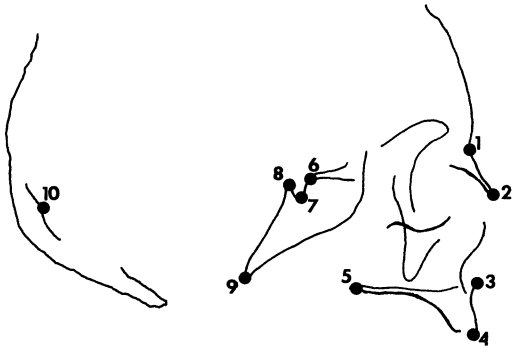

FIG. 1. Two-dimensional landmarks used in analysis of Crouzon, Apert and normal faces plotted on a lateral projection of the human skull. See Table 1 for description of landmarks.

ble 1 and Fig. 1) located on lateral radiographs of children at 4 and 13 years of age. Sample sizes are as follows:

Sample	Age	
	4 yr	13 yr
Crouzon syndrome	5	5
Apert syndrome	4	5
Normal	20	19

The other two data sets consist of three-dimensional coordinates of landmark locations. Three-dimensional data were collected by a single observer using the 3Space digitizer (Polhemus Navigation, see Hildebolt and Vannier, 1989).

The first of the 3-D data sets consists of coordinates of 18 homologous landmarks located on the facial skeleton of a species of Old World monkeys, *Macaca fascicularis*, and a species of New World monkeys, *Cebus apella*. All specimens considered are male and come from the collections of the National Museum of Natural History, Smithsonian Institution. The specimens were aged according to tooth eruption patterns. Data from two developmental age categories are used here: immature (having only deciduous teeth); and adult (having

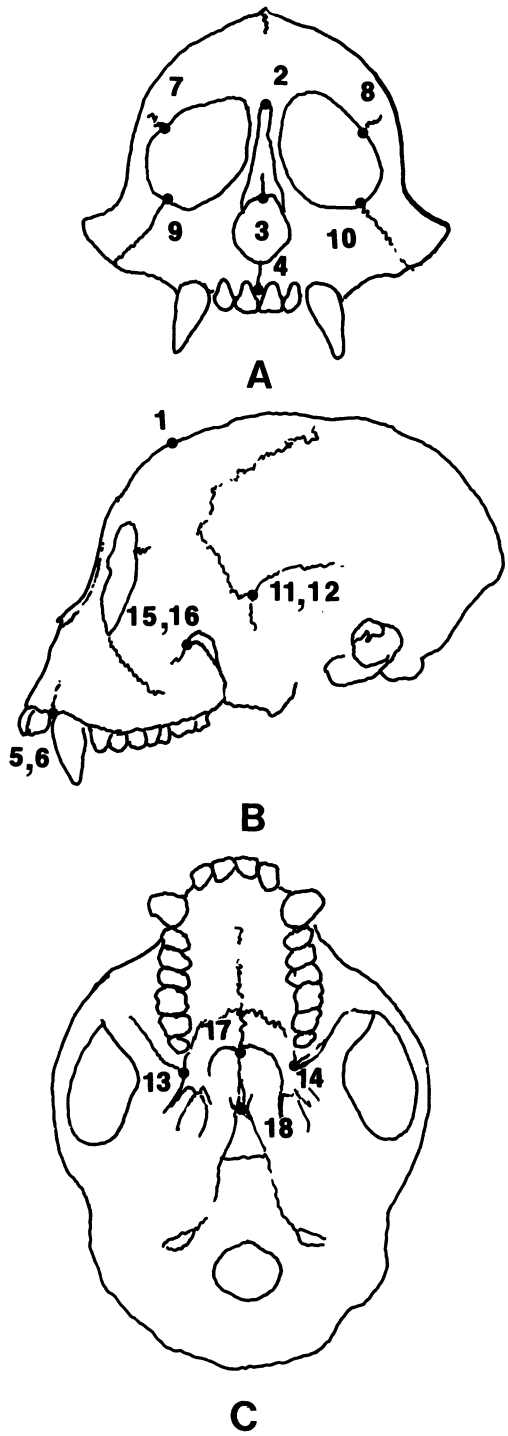

→

FIG. 2. Three-dimensional landmarks used in analysis of *Cebus apella* and *Macaca fascicularis*. Landmarks are plotted on line drawings of *C. apella* showing frontal (A), lateral (B), and inferior (C) views. See Table 2 for description of landmarks.

TABLE 2. Three-dimensional landmarks used in analysis of *Cebus apella* and *Macaca fascicularis*.

Landmark number	Landmark name and description
1	Point located midway along the arc measured along the neurocranial surface from bregma to nasion.
2	Nasion. Point of intersection of the nasal bones with the frontal bone.
3	Nasale. Inferior-most point of intersection of the nasal bones.
4	Intradentale superior. The point is located on the alveolar border of the maxilla between the central incisors.
5	Right junction of premaxilla and maxilla on alveolar surface.
6	Left junction of premaxilla and maxilla on alveolar surface.
7	Right junction of the frontal bone with the zygomatic bone on the orbital rim.
8	Left junction of the frontal bone with the zygomatic bone on the orbital rim.
9	Right zygomaxillare superior. Intersection of zygomatic bone and maxilla at the inferior orbital rim.
10	Left zygomaxillare superior. Intersection of zygomatic bone and maxilla at the inferior orbital rim.
11	Right pterion posterior. Intersection of the frontal (in *M. fascicularis*, parietal in *C. apella*), sphenoid, and temporal bones.
12	Left pterion posterior. Intersection of the frontal (in *M. fascicularis*, parietal in *C. apella*), sphenoid, and temporal bones.
13	Right maxillary tuberosity. Intersection of the maxilla and the palatine bones at alveolar ridge.
14	Left maxillary tuberosity. Intersection of the maxilla and the palatine bones at alveolar ridge.
15	Intersection of the zygomatic, maxillary, and sphenoid bones at the pterygo-palatine fossa on the right side.
16	Intersection of the zygomatic, maxillary, and sphenoid bones at the pterygo-palatine fossa on the left side.
17	Posterior nasale spine. Posterior-most point of intersection of the right and left palatal shelves.
18	Junction of the vomer and sphenoid bone on the sphenoid body.

a complete permanent dentition). The landmarks considered are defined in Figure 2 and Table 2, and sample sizes are as follows:

Species	Developmental age category	
	Immature	Adult
Macaca fascicularis	12	20
Cebus apella	12	20

The second of the 3-D data sets contains landmark coordinates collected from the craniofacial complex of New Zealand rabbits (*Oryctolagus cuniculus*) raised in a laboratory setting. All specimens were sacrificed at 18 and one-half weeks of age. We consider 18 landmarks (see Table 3, Fig. 3). The sample consists of eight male individuals.

STATISTICAL ANALYSIS

Each data set was analyzed using generalized procrustes analysis as described in Goodall and Bose (1987). This technique produces a consistent estimate of the mean shape, X, and the standard deviation, ϵ.

Initially, each form was split into two sections such that there were no landmarks common to both parts. We then estimated the variability, ϵ, for each section using the generalized procrustes statistic, G_S. Since the two sections have no landmarks in common, it can be shown that under model (1), the two G_S statistics are independent, χ^2 random variables with degrees of freedom d_1 and d_2, respectively. The value of $d_i (i = 1, 2)$ is given by:

$$d_i = [N_i K - \tfrac{1}{2}K(K + 1) - 1](L - 1)$$

where N_i is the number of landmarks in the i^{th} section and K is the dimension and L is the sample size. See Goodall and Bose (1987) for the corresponding derivations. It follows that

$$F = \frac{G_S^1/d_1}{G_S^2/d_2} \text{ has } F_{d_1,d_2} \text{ distribution}$$

TABLE 3. Three-dimensional landmarks used in analysis of *Oryctolagus cuniculus*. Landmark numbers are not consecutive because this data represents a subset of a larger data set.

Landmark number	Landmark name and description
1	Nasale. Intersection of distal end of nasal bones at nasal suture.
2	Nasion. Intersection of proximal end of nasal bones at internasal and interfrontal suture.
3	Most lateral edge of naso-frontal suture at junction with incisive bone, right side.
4	Most lateral edge of naso-frontal suture at junction with incisive bone, left side.
12	Lambda. Intersection of sagittal suture with interparietal bone.
13	Right asterion. Most lateral projection of interparietal bone at junction with parietal bone, right side.
14	Left asterion. Most lateral projection of interparietal bone at junction with parietal bone, left side.
15	External occipital protuberance at midline.
16	Right edge of external occipital protuberance.
17	Left edge of external occipital protuberance.
18	Distal junction of naso-incisive suture, right side.
19	Distal junction of naso-incisive suture, left side.

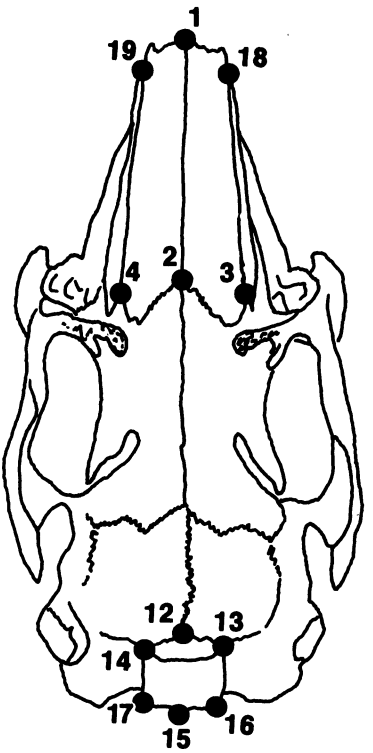

FIG. 3. Three-dimensional landmarks used in analysis of *Oryctolagus cuniculus* projected onto a two-dimensional view of the rabbit skull from above. See Table 3 for description of landmarks.

where G_S^i denotes the G_S statistic corresponding to the i^{th} part.

Intuitively, we expect that variability for landmarks that are located close together is less than for landmarks that are farther apart. We used this intuition to decide the splitting of biological forms into two parts.

Results of our analysis for equality of variances in all three samples are displayed in Table 4. In each case, the hypothesis of equality of variances is strongly rejected.

Following the suggestion of the anonymous referee, we calculated the variability of assorted subgroups of landmarks on the skulls of *Oryctolagus cuniculus*. Landmarks delimiting the intersection of the nasal bones with the frontal bones (2, 3, 4) are most variable, while landmarks at the most anterior aspect of the nasal bones (1, 18, 19) and those on the occipital protuberance (12, 13, 14, 15, 16, 17) have similar but low variances, 0.03439 and 0.03491, respectively.

We might expect those landmarks that are most centrally located (2, 3, 4 in this example) to have the lowest variance due to the constraints of a rotational fitting procedure. However, our results are contrary to this expectation and underscore the importance of biological constraints (e.g., developmental, structural, functional) on anatomical design.

Our proposed biological reasons for the low variances determined for the most anterior and the most posterior groups of landmarks differ between groups. The more anterior group of landmarks (1, 18, 19) defines the anterior border of the paired nasal bones. We feel that the variance is comparatively low here because the location of these landmarks are dependent on a single

TABLE 4. Analysis for equality of variances in three data sets.

Data Set I					
	Landmarks 6, 7, 8		Landmarks 1, 2, 3, 4, 5, 9, 10		F-Ratio
	$\hat{\epsilon}_1$	*df*	$\hat{\epsilon}_2$	*df*	$\hat{\epsilon}_1^2/\hat{\epsilon}_2^2 = F$
(1) Normal children					
Age 4	0.04676	38	0.52893	190	127.95
Age 13	0.05849	36	0.19260	180	10.84
(2) Apert Syndrome					
Age 4	0.05125	6	0.34077	30	44.21
Age 13	0.06411	8	0.31433	40	24.04
(3) Crouzon Syndrome					
Age 4	0.06181	8	0.26144	40	17.89
Age 13	0.09326	8	0.36119	40	15.00
Data Set II					
	Landmarks 4, 5, 6		Landmarks 1–3, 7–18		F-Ratio
	$\hat{\epsilon}_1$	*df*	$\hat{\epsilon}_2$	*df*	$\hat{\epsilon}_1^2/\hat{\epsilon}_2^2 = F$
M. fascicularis					
Age 1	0.04395	22	0.10428	418	5.63
Age 5	0.08784	38	0.13581	722	2.39
C. apella					
Age 1	0.05692	22	0.08466	418	2.21
Age 5	0.07196	38	0.12079	722	2.82
Data Set III					
	Landmarks 12–17		Landmarks 1–4, 18, 19		F-Ratio
	$\hat{\epsilon}_1$	*df*	$\hat{\epsilon}_2$	*df*	$\hat{\epsilon}_1^2/\hat{\epsilon}_2^2 = F$
Oryctolagus cuniculus					
	0.03491	77	0.06767	77	3.76

pair of bones and are not affected or constrained by contact with other osseous elements. The more posterior group of landmarks (12, 13, 14, 15, 16, 17) outlines an area of nuchal muscle attachment. Like the landmarks that describe the most anterior portion of the nasal bones, landmarks 15, 16, and 17 lie on a single bone. Moreover, the morphology required for effective muscle attachment in this region may limit the amount of variation that is possible before the design becomes functionally unsound.

The landmarks located centrally in our biological configuration (2, 3, 4) show the greatest amount of variation in location. We believe that this simply reflects dynamics of sutural biology. Landmarks 2, 3, and 4 are situated at the intersection of either three or four independent bones. Because sutural morphology is dependent upon the approximation of adjacent bony boundaries, the variability of sutural intersections (in our example, landmark locations) will increase with the number of bones involved in the formation of this boundary. Since the formation of particular articulating bones may be dependent upon the growth of independent soft tissue functioning matrices (sensu Moss, 1973), we can expect a great degree of variability for landmarks that mark the intersection of several bony elements. This variability may be greater or less depending upon which bony structures are involved and upon which soft tissue components their growth patterns depend.

The second part of the analysis considers only the first data set consisting of 2-D landmark data from the human craniofacial complex. In Table 5 we compare the estimate of ϵ as obtained from GPA of the complete craniofacial complex with the minimum distance between any pair of

TABLE 5. Comparison of $\hat{\epsilon}$ with the minimum distance between any pair of landmarks.

Data set	$\hat{\epsilon}$	Minimum distance*
Crouzon Syndrome—Age 4	0.32946	0.62
Apert Syndrome—Age 4	0.30876	0.63
Normal children—Age 4	0.43546	0.54

* The minimum distance corresponds to the minimum of all possible distances among 10 landmarks in the average form X as obtained by GPA after rotation and scaling.

landmarks. It is clear from Table 5 that the calculated values of ϵ could easily (and realistically) cause any of the closely spaced landmarks to switch their positions. However, this is biologically impossible. The minimal distance was consistently found among landmarks 6, 7 and 8 which define the limits of the pituitary fossa.

We have demonstrated that the assumption of homoscedasticity of variances is unrealistic in three biological situations. There may be situations where it holds true but, for general applications, this assumption is both constraining and unrealistic.

ALTERNATIVE MODELS

Since we have demonstrated the inadequacy of the perturbation model with variance-covariance matrix $\epsilon^2 I$, the problem remains to develop a realistic and practical model for the analysis of morphometric data, in particular, landmark data. Below we discuss two alternative models that have been proposed in the literature. Finally, we specify the key characteristics required of a proper statistical model for landmark data.

Goodall and Bose Model

Realizing the need for a more general variance-covariance matrix for the perturbation distribution, Goodall and Bose (1987) suggest the following model for the perturbations E_i:

$$E_i \sim MN(O, \Sigma_N \times \Sigma_K)$$

where MN denotes matrix valued normal distribution, Σ_N is a positive definite, symmetric $N \times N$ matrix and Σ_K is another positive definite, symmetric $K \times K$ matrix; $\times$ denotes the Kronecker product. $\Sigma_N \times \Sigma_K$ is the variance-covariance matrix of E_i and O is the mean. There are two major problems associated with this model.

First, the number of parameters is extremely large, namely

$$\frac{N(N+1)}{2} + \frac{K(K+1)}{2}.$$

Clearly, to estimate the parameters reasonably well one would need fairly large samples. Whether such large samples are available or not depends on the particular study. However, sample size is commonly limited in biological studies and this model will therefore be difficult to use. The use of parametric models for Σ_N and Σ_K might reduce the number of parameters but it is not clear which parametric models are realistic.

Second, and more critically, even in cases where sample size is sufficient, the variance-covariance matrix, Σ_N, cannot be consistently estimated using landmark data.

Let us consider the simplest situation where there is no scaling or rotation. Following the notation of the previous section, let

$$X_i = X + E_i + 1_N t_i',$$

Let us also assume that Σ_K is identity matrix I_K. Goodall (1989) assumes such a structure. (Note this assumption is biologically unrealistic since it says that landmarks vary independently of each other along different axes but are correlated along a fixed axis. Notwithstanding, we will allow it for the sake of simplicity.) Then

$$X_i \sim MN(X + 1_N t_i', \Sigma_N \times I_K). \quad (*)$$

Note that since each observation gets shifted by an unknown and different translation parameter t_i', the number of unknown parameters, namely, (X, t_i, Σ_N), goes to infinity at the same rate as the number of observations. This phenomenon belongs to the class of problems dealing with infinitely many nuisance parameters. (See particularly Example 2 on page 4 of Neyman and Scott, 1948.) Our aim is to estimate X and Σ_N; t_i's are nuisance parameters.

In the univariate case the situation can

be stated as follows: X_i's are independent normal random variables with mean $\mu \times t_i$ and variance σ^2 and we want to estimate μ and σ^2 consistently: t_i's are nuisance parameters.

It is well known that in this situation σ^2 is not estimable in general. One can estimate σ^2 if there are at least two observations with the same nuisance parameter or if t_i's are themselves random variables having common distribution. Both these situations are unrealistic in any biologically based morphological studies. Hence, under the model described in (*), Σ_N is non-estimable.

In the following exercise, we show that under some reasonable conditions, X, the mean form, can be estimated consistently but the parameter of interest Σ_N cannot be estimated. Consider the model in (*). Assume that the average form X is such that the columns sum to zero: that is, the average form is centered. Let us transform the observations X_i's such that they are centered: that is, the columns sum to zero. Then these transformed observations, X_i^*'s, have the following distribution

$$X_i^* \sim MN(X, \Sigma_N^* \times I_K)$$

where X is the mean and Σ_N^* is the variance-covariance matrix. Note also that X_i^*'s are now independent and also identically distributed with the average form X as the mean. It is obvious that $\bar{X}^*$, the average of X_i^*'s, estimates X — the average form consistently. It is also clear that the sample variance-covariance matrix can be used to estimate Σ_N^*. However, note that Σ_N^* is not the same as Σ_N. Σ_N^* is a singular matrix of rank $(N - 1)$, one less than that of Σ_N. This follows because centering of the observations imposes a linear constraint on the entries in the columns of X_i^*, reducing the rank by one. By using X_i^*'s and $\bar{X}^*$ one can estimate Σ_N^* consistently, but Σ_N, the parameter of interest, cannot be estimated consistently. Our point becomes more obvious in the univariate case:

$$X_i \sim N(\mu + t_i, \sigma^2), \qquad \sigma^2 > 0.$$

In this case, a centered form is equivalent to having μ equal to 0. One centers the observation X_i by subtracting X_i from it, (i.e., $\bar{X}^*$) is identically equal to zero. Thus, equal to zero for all i. The mean of X_i^*'s (i.e., $\bar{X}^*$) is identically equal to zero. Thus, the mean μ is estimated correctly to be 0. However, since the variance of X_i^*'s is exactly zero (they are degenerate at zero), the variance of X_i^*'s does not estimate σ^2 (>0) correctly. In fact, σ^2 is non-estimable! Note X_i^*'s are in the space of rank zero, one less than that of X_i's.

The conclusion of this discussion is that the general model proposed in Goodall and Bose (1987) is unrealistic since the parameters of interest are non-estimable.

Mosimann's Models

Mosimann (1970, 1975a, b) suggests the use of linear distances to study populations of forms. He develops characterization theorems for lognormal and some other positive random variables. Bookstein (1978) and Bookstein et al. (1985) criticize Mosimann's approach as being non-geometric and therefore inadequate because Mosimann does not consider distances between homologous landmarks. In this section, we critique Mosimann on other grounds, regardless of whether the distances considered are landmark based or not.

First, Mosimann does not offer any biologically sensible statistical mechanism (such as the perturbation mechanism described earlier) to account for the landmark distances having a Lognormal, Gamma or Dirichlet distribution. These distributions are chosen more for statistical convenience than biological reality. Second, Mosimann does not clearly prescribe how many distances should be taken to preserve all the information about the form of the object. Moreover, he does not state how these distances should be stochastically related. Clearly, they cannot be independent of each other. But how do we characterize the variance–covariance matrix? What is the rank of this variance–covariance matrix? Unless these questions are answered satisfactorily, it is not clear why these distributions should model the vector of linear distances realistically.

TOWARDS A REASONABLE STATISTICAL MODEL OF BIOLOGICAL FORM

An essential characteristic of a statistical model for populations of biological objects is that every observation generated by the statistical model should at least correspond to an object in the appropriate dimension, either two or three. It is clear that the perturbation model proposed by Bookstein satisfies this requirement. The following discussion is applicable when one uses linear distances between biological landmarks.

In Lele (1989) it is shown that to represent an object with N landmarks one can use $N(N-1)/2$ distances. Only certain proper subsets of these distances are sufficient. Moreover, it is also shown that the space of all two-dimensional objects represented by N landmarks corresponds to the space of all $N \times N$ symmetric positive semidefinite matrices of rank two. For three-dimensional objects the rank of the matrix is necessarily three. It is clear that the statistical model for the $(N \times N)$ matrix of all linear distances (which represents the form of the object as described by N landmarks completely) take values in the space of all $N \times N$ positive semidefinite matrices of proper rank, either 2 or 3.

Note that the range of the statistical models proposed by Mosimann is bigger than the allowed range. Thus, these models can generate objects which exist in four or higher dimensions; in fact, they may not necessarily correspond to any geometrical object at all! For example, if one uses a three-variate lognormal distribution with mean vector (1, 1, 1), it is possible to get an observation (1.5, 0.8, 0.6). This observation vector does not correspond to a triangle on a plane even though the mean vector does! We feel that statistical procedures developed using such models should be approached with care.

Another characteristic of a good statistical model is that the parameters be estimable. We have shown that for perturbation models some of the parameters of interest (such as variance-covariance matrix) may not be estimable due to the existence of nuisance parameters corresponding to translation. It is not clear how rotation and scaling affect the estimability, and hence the statistical testing procedures based on these.

DISCUSSION

We have illustrated that the perturbation models with variance-covariance matrix $\epsilon^2 I$ are unrealistic on biological grounds, whereas the general model with variance-covariance matrix $(\Sigma_N \times I_K)$ or $(\Sigma_N \times \Sigma_K)$ leads to non-estimability of the parameter of interest, namely, Σ_N. Models for linear distances such as Lognormal, Gamma or similar positive valued random variables do not necessarily generate observations which correspond to a geometrical object in proper dimensions, either 2 or 3. Our work underscores the need for statistical methods that are less model dependent than the existing ones.

We stress that data used in this study were collected for other purposes. They were not chosen as counter examples, nor do they represent exceptional biological data sets. The actual morphology of the object dictates the availability and location of landmarks. For example, due to the morphology of osseous elements of the skull, there are particular regions that offer more landmarks to the researcher. The cranial base is a region where a number of separate bones come together to form a functioning unit which supports the brain and transmits major neurovascular bundles. This region offers a multitude of landmarks and, because of the comparatively compact size of the region, the landmarks are closely spaced. The neurocranium, on the other hand, is characterized by a few, large bony elements with smooth surfaces and few foramina. Since few landmarks are available to describe this comparatively large biological region, the distribution of neurocranial landmarks will be diffuse.

Variability of a landmark not only depends on its position relative to its neighbors but also on the inherent structure of the landmark. For example, we have found landmarks based on suture intersections in

the pterion region (i.e., various intersections of frontal, sphenoidal, zygomatic and parietal bones) to be highly variable (Richtsmeier and Danahey, unpublished data), while landmarks that mark the intersection of two sutures at a border (e.g., nasale, intradentale superior) show relatively little variability. It is interesting to consider the evolutionary implications of the pterion region in conjunction with its predisposition to high variability in location, but these ideas await further analyses. When comparing forms which differ as the result of a biological process (e.g., evolution, growth, teratological factors), we suggest that the biologist might offer some expectations regarding the degree of local variability based on knowledge of the biological forms under study and the particular process responsible for change. Incorporating this information into statistical models has not been attempted, but could prove useful.

Biology has presented us with a number of constraints on the description of form by landmark data based solely on architecture. It seems unwise to place additional constraints on analyses that are based on statistical models.

ACKNOWLEDGMENTS

Use of skeletal collections of the NMNH was kindly allowed by Dr. Richard Thorington, Division of Mammals, Smithsonian Institution. We thank Tom Broad and Steve Danahey for assistance in data collection. Rabbits used in this study were part of a larger study under the direction of Dr. Craig Dufresne, The Johns Hopkins University. This work was supported in part by a Basil O'Connor grant from the March of Dimes Birth Defects Foundation, a biomedical research grant from the Whitaker Foundation and BRSG Grant No. 2-S07-RR05445-27.

We are grateful to the Associate Editor, Professor Michael Douglas, for his kind support and encouragement. We acknowledge Fred Bookstein and the other anonymous referee for their comments.

REFERENCES

BOOKSTEIN, F. L. 1978. The measurement of biological shape and shape change. Lecture Notes in Biomathematics 24. Springer, Berlin.

BOOKSTEIN, F. L. 1984. A statistical method for biological shape comparisons. J. Theor. Biol., 107:475–520.

BOOKSTEIN, F. L. 1986. Size and shape spaces for landmark data in two dimensions. Stat. Sci., 1(2): 181–242.

BOOKSTEIN, F. L. 1989a. Discussion of Kendall's paper. Statist. Sci., 4:99–105.

BOOKSTEIN, F. L. 1989b. Principal warps: Thin plate splines and the decomposition of deformations. IEE Trans. Pattern Anal. Machine Intelligence, 11, 567–585.

BOOKSTEIN, F., B. CHERNOFF, R. ELDER, J. HUMPHRIES, G. SMITH, AND R. STRAUSS. 1985. Morphometrics in evolutionary biology. Special Publication 15, The Academy of Natural Sciences of Philadelphia.

BROADBENT, B. H., BROADBENT, B. H. JR., AND W. H. GOLDEN. 1975. Bolton standards of dentofacial developmental growth. C. V. Mosby, St. Louis.

GOODALL, C., AND A. BOSE. 1987. Models and procrustes methods for the analysis of shape differences. Proc. 19th Symp. Interface between Computer Science and Statistics.

GOODALL, C. 1989. WLS estimators and tests for shape differences in landmark data. Technical Report, Program in Statistics and Operations Research, Princeton University, Princeton, New Jersey.

HILDEBOLT, C. F., AND M. W. VANNIER. 1988. Three-dimensional measurement accuracy of skull surface landmarks. Amer. J. Phys. Anthropol., 76:497–503.

LELE, S. R. 1989. Some comments on coordinate-free and scale invariant methods in morphometrics. Submitted for publication.

MOSIMANN, J. E. 1970. Size allometry: Size and shape variables with characterisations of the lognormal and generalized gamma distributions. J. Amer. Statist. Assoc., 65:930–978.

MOSIMANN, J. E. 1975a. Statistical problems of size and shape. I. Biological applications and basic theorems. Pages 187–217 *in* Statistical distributions in scientific work. Volume 2 (G. P. Patil et al., eds.). D. Reidel Publishing Company, Holland.

MOSIMANN, J. E. 1975b. Statistical problems of size and shape. II. Characterisations of the lognormal, gamma and dirichlet distributions. Pages 219–239 *in* Statistical distributions in scientific work. Volume 2 (G. P. Patil et al., eds.). D. Reidel Publishing Company, Holland.

MOSS, M. L. 1973. A functional cranial analysis of primate craniofacial growth. Pages 198–208 *in* Symp. IVth Int. Congr. Primat. Volume 3: Craniofacial biology of primates.

NEYMAN, J., AND E. L. SCOTT. 1948. Consistent estimates based on partially consistent observations. Econometrica, 16:1–32.

RICHTSMEIER, J. T. 1985. A study of normal and pathological craniofacial morphology and growth using finite element methods. Ph.D. dissertation, Northwestern University, Evanston, Illinois.

Received 29 June 1989; accepted 3 January 1990